Electronic Supplementary Material (ESI) for ChemComm.
This journal is © The Royal Society of Chemistry 2017

Supporting Information

Amorphous/Crystalline Hybrid MoO_2 Nanosheets for High-Energy Lithium-Ion Capacitors

Xu Zhao, [a, b] Hong-En Wang, [c] Jian Cao, [a] Wei Cai, [b] Jiehe Sui * [a]

[a] State Key Laboratory of Advanced Welding and Joining, Harbin Institute of Technology, Harbin 150001, China

[b] School of Materials Science and Engineering, Harbin Institute of Technology, Harbin, 150001, China.

[c] State Key Laboratory of Advanced Technology for Materials Synthesis and Processing, Wuhan University of Technology, 122 Luoshi Road, 430070 Wuhan, Hubei, China.

Corresponding Author: Prof. Jiehe Sui, email: suijiehe@hit.edu.cn

Experimental Section

Preparation of crystalline/amorphous MoO_2:

MoO_2 was obtained via a solvothermal reaction. In brief, 0.6 g commercial Molybdenum trioxide (MoO_3, Sinopharm, AR) was dispersed into water and ethylene glycol (EG, Sinopharm, > 98 %) at room temperature under stirring for 1 h. After that, the mixture was transferred into a 100 mL Teflon stainless steel autoclave, sealed and maintained at desired temperature (160, 180 and 200 ℃) for 12 h. After cooling down to room temperature, the solution with powders was filtered and washed with absolute ethanol three times (Sinopharm, 99 %) and dried at 70 ℃ in vacuum for 6 h.

Material characterizations:

The phase structure was analyzed by XRD with a PANalytical X'Pert Pro X-ray diffractometer using Cu Kα radiation (1.54056 Å). The morphology was examined using scanning electron microscopy (SEM, FEI Helios Nanolab 600 I). TEM was carried out using an FEI Tecnai G2 F30.

CR 2032 coin-type cells were assembled for electrochemical measurements. The positive electrodes were fabricated by casting a slurry consisting of as-prepared MoO_2 (80 wt %), acetylene black (10 wt %) and poly (vinylidene fluoride) (PVDF, 10 wt %) dispersed in N-methyl-2-pyrrolidone (NMP) onto a copper foil with a doctor blade, followed by drying at 80 ℃ under vacuum overnight. Electrodes were punched into discs with diameter of 8 mm. A lithium metal foil and a Celgard M-824 membrane were used as a counter electrode and a separator, respectively. Lithium ion capacitors were fabricated in which commercial activated carbon was employed as cathodes (coating on Al foil) and MoO_2 electrodes as anodes. In the process of capacitor fabrication, MoO_2 anode was firstly experienced three cycles under 0.05 A g^{-1} in the voltage range of 1.0 ~ 3.0 V. Then the cell was discharge to 1.0 V and subsequently disassembled. M-824 separator was set between anode and cathode. Electrolyte for both LIB half cell and LIC were 1 M $LiPF_6$ in ethylene carbonate (EC)-dimethyl carbonate (DMC) (1:1, vol % Novolyte Tech., Suzhou). The cells were operated in an Ar-filled glove box with O_2 and H_2O lower than 0.5 ppm. All the tests are performed at room temperature. Cyclic voltammetry (CV) curves were recorded on a CHI 650 B electrochemical workstation. Galvanostatic charge-discharge (GCD) tests was recorded on the battery tester (LAND CT2001A, China). The electrochemical impedance spectra (EIS) were obtained using a potentiostat (Autolab PGSTAT-302N, Netherland) by applying an AC voltage of 5 mV over the frequency range from 0.01 Hz to 100 kHz. The specific energy and specific power densities of Li-ion capacitors were calculated as follows:

$$E = \int_{t1}^{t2} IVdt = \Delta V \frac{I}{m} t$$

$$P = \frac{E}{t} = \Delta V \frac{I}{m}$$

$$\Delta V = V_{max} - V_{min}$$

Where E (Wh kg^{-1}) is energy density, P (W kg^{-1}) is power density, I is the constant current (A), t_1 and t_2 is the start time and end time in the discharge process, V_{max} is the potential at the beginning of discharge after the IR drop, V_{min} is the terminal voltage in the discharge process. The energy density and power density of SICs against the two electrodes in device were calculated based on the total mass of the active materials in anode and cathode.

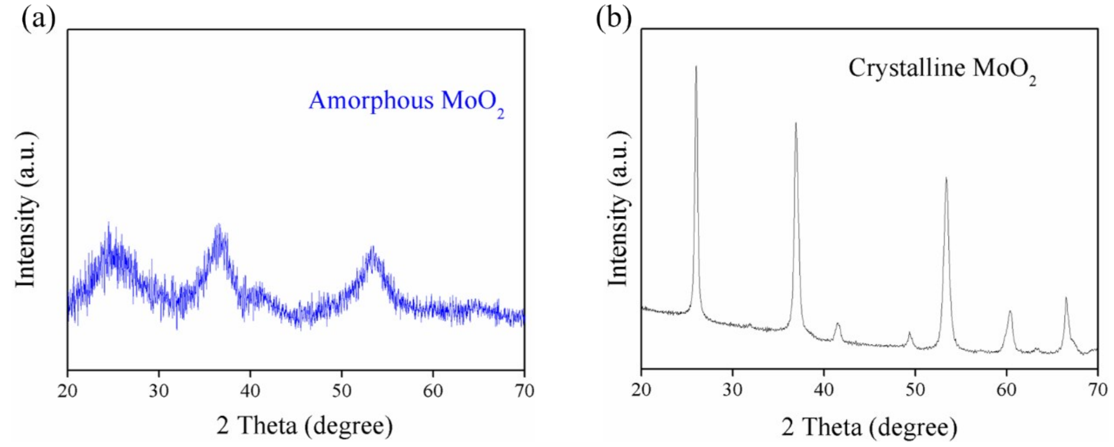

Fig. S1. XRD patterns of (a) amorphous and (b) crystalline MoO_2.

The possible mechanism for synthesizing MoO_2 using MoO_3 as precursor and ethylene glycol as reducing agent at high temperature (160, 180 and 200 ^{o}C) for 12 h can be concluded as following:

$$HO\text{-}CH_2\text{-}CH_2\text{-}OH + MoO_3 \rightarrow O{=}CH_2\text{-}CH_2{=}O + MoO_2 + H_2O \quad (\textbf{Eq. S1})$$

At a relative low temperature (e. g. 160 ^{o}C), XRD pattern of as-prepared product exhibits broadened diffraction peaks that can be well indexed to pure MoO_2 without other impurities such as MoO_3 precursor. With the increase of synthesis temperature, the diffraction peaks gradually become intense and sharp, which can be attributed to the improvement of crystallinity. Based on this, we investigate the relationship between the FWHMs and intensities in samples from amorphous to crystalline. The enhanced intensity and decreased FWHM demonstrated that the higher degree of crystallinity in samples was obtained with the increase of solvothermal temperatures.

Table S1. FWHM and intensities of the (-1 1 1) peak.

Sample ID	Synthesis temperature (°C)	FWHM (°)	Intensity (a.u.)
Amorphous MoO_2	160	0.94	137
Discrepant MoO_2	180	0.74	726
Crystalline MoO_2	200	0.35	3095

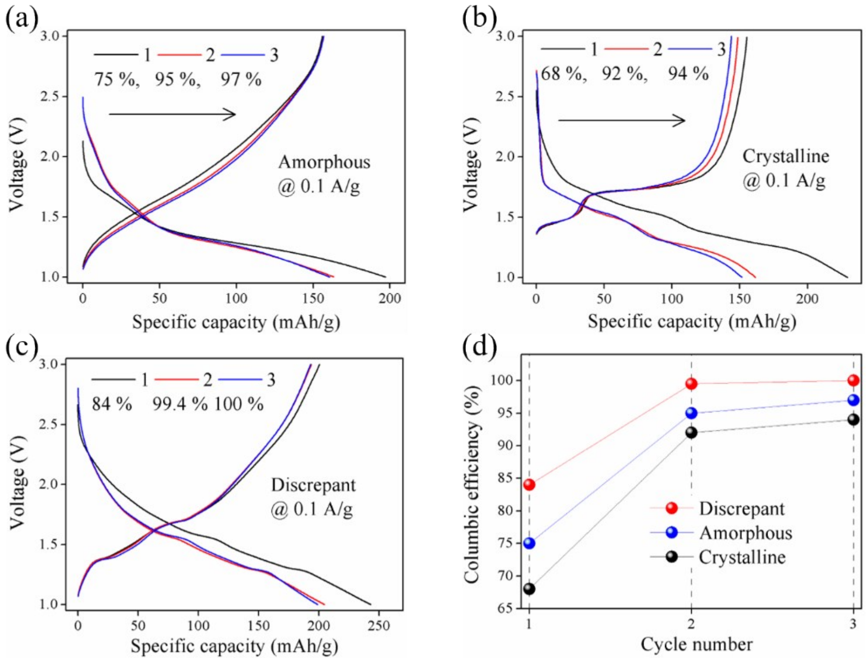

Fig. S2 GCD profiles of (a) amorphous MoO_2, (b) crystalline MoO_2 and (c) discrepant MoO_2; (d) Coulombic efficiencies in first three cycles.

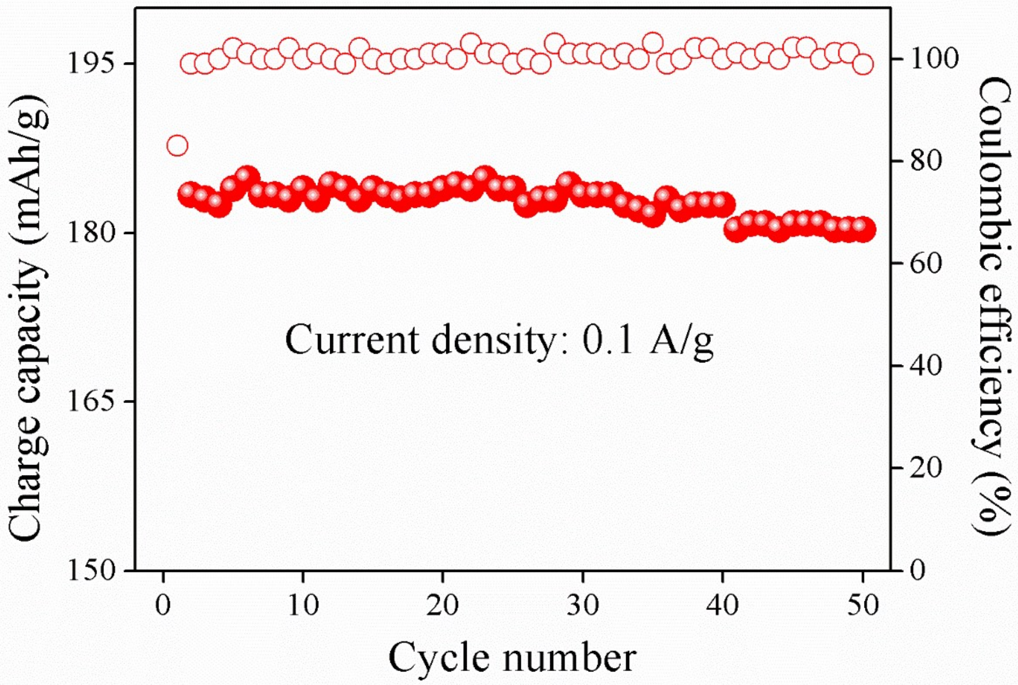

Fig. S3 Cycling performance and corresponding coulombic efficiency of discrepant MoO_2 electrode at a current density of 0.1 A/g.

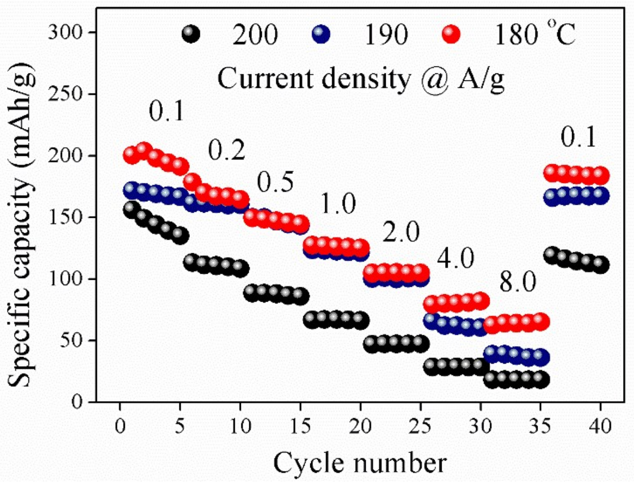

Fig. S4 LIB performance comparison of MoO_2 synthesized at 180, 190 and 200 °C.

The amorphous/crystalline heterostructures could be obtained through controlling solvothermal temperature. The existence of amorphous/crystalline heterostructure can potentially increase the lithium storage capability of the MoO_2 anodes. Based on this, the ratio between the crystalline and amorphous phase could be adjusted through controlling the temperature. For example, samples prepared at 190 °C is expected to have more crystallinity. The rate performance is shown in **Fig. S4**, which is inferior than discrepant MoO_2 (prepared at 180 °C) but superior than that of crystalline MoO_2 (prepared at 200 °C), which could be attributed to the synergistic effect of crystalline and amorphous heterostructure.

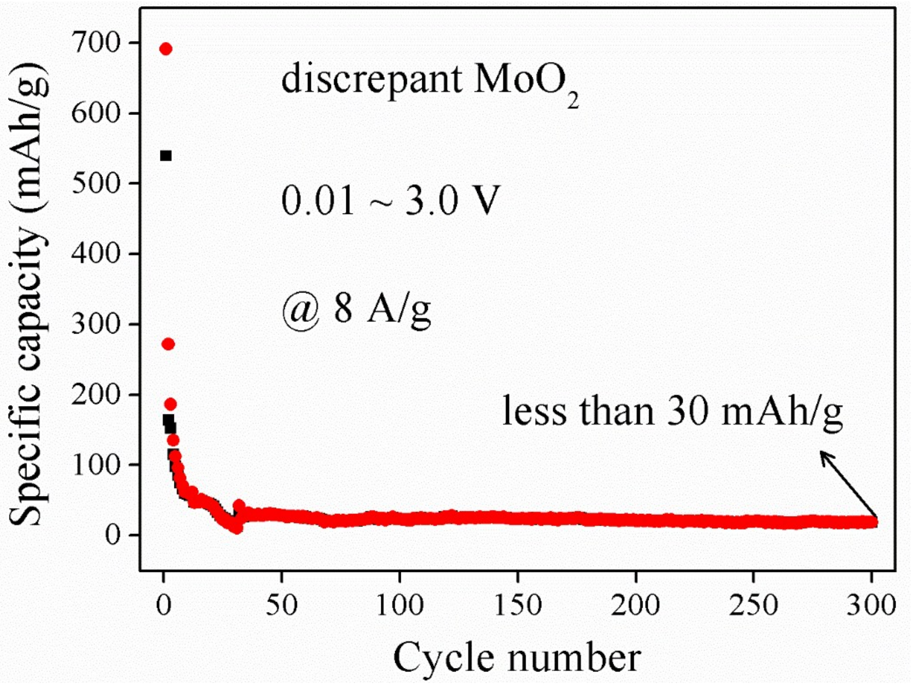

Fig. S5. Cycling performance of discrepant MoO_2 electrode at 8 A g^{-1} in the voltage range of 0.01 ~ 3.0 V.

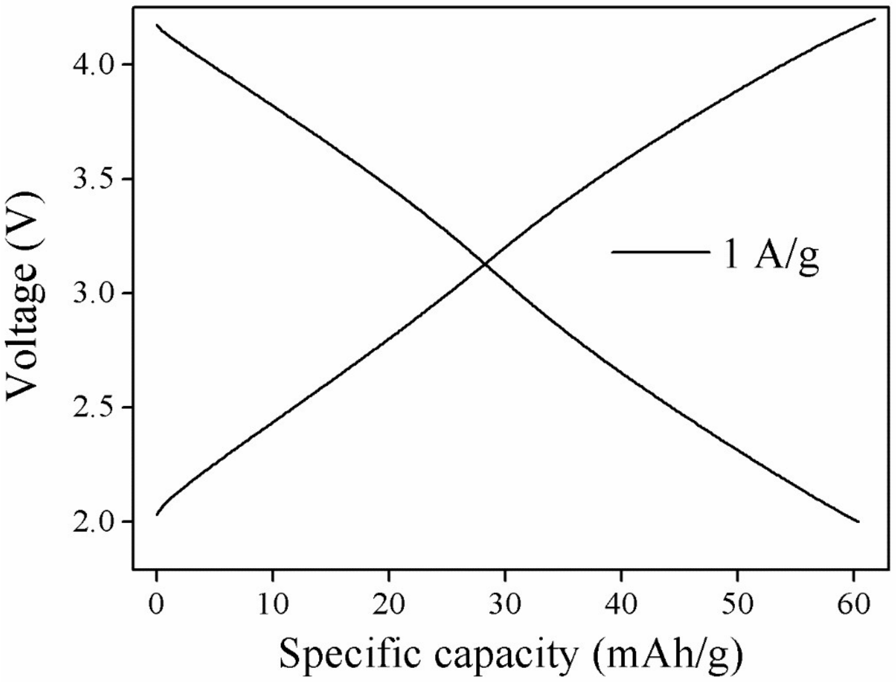

Figure S6. The charge/discharge curves of activated carbon cathode at current density of 1 A g^{-1} the voltage window of 2.0 ~ 4.2 V. The linear charge or discharge profiles indicate AC in Li in device with an EDLC mechanism to store energy. All data are measured from half-cells where Li metals are used as counter electrodes.

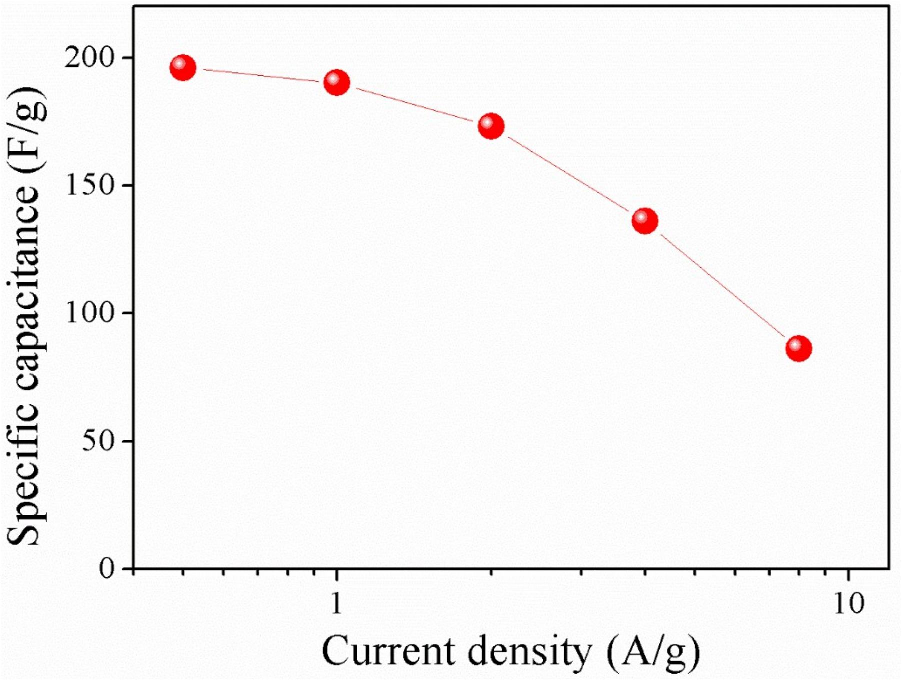

Fig. S7. Specific rate capacitances of LICs device based on discrepant MoO_2 anode.

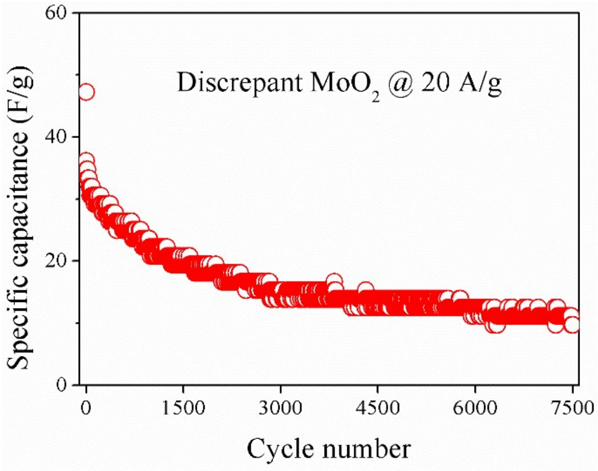

Fig. S8 Long-term cycling performance of the discrepant MoO_2 || AC device tested at 20 A/g.